

# Stock markets reconstruction via entropy maximization driven by fitness and density

Tiziano Squartini,<sup>1,2</sup> Guido Caldarelli,<sup>1,2,3</sup> and Giulio Cimini<sup>1,2,\*</sup>

<sup>1</sup>*IMT School for Advanced Studies, Piazza S.Francesco 19, 55100 Lucca - Italy*

<sup>2</sup>*Istituto dei Sistemi Complessi (ISC)-CNR, Via dei Taurini 15, 00185 Rome - Italy*

<sup>3</sup>*London Institute for Mathematical Sciences, 35a South Street, W1K 2XF London - United Kingdom*

(Dated: March 12, 2018)

The spreading of financial distress in capital markets and the resulting systemic risk strongly depend on the detailed structure of financial interconnections. Yet, while financial institutions have to disclose their aggregated balance sheet data, the information on single positions is often unavailable due to privacy issues. The resulting challenge is that of using the aggregate information to statistically reconstruct financial networks and correctly predict their higher-order properties. However, standard approaches generate unrealistically dense networks, which severely underestimate systemic risk. Moreover, reconstruction techniques are generally cast for networks of bilateral exposures between financial institutions (such as the interbank market), whereas, the network of their investment portfolios (i.e., the stock market) has received much less attention. Here we develop an improved reconstruction method, based on statistical mechanics concepts and tailored for bipartite market networks. Technically, our approach consists in the preliminary estimation of connection probabilities by maximum-entropy inference driven by entities capitalizations and link density, followed by a density-corrected gravity model to assign position weights. Our method is successfully tested on NASDAQ, NYSE and AMEX filing data, by correctly reproducing the network topology and providing reliable estimates of systemic risk over the market.

PACS numbers: 89.75.Hc; 89.65.Gh; 02.50.Tt

The recent financial crises have stressed the critical importance of correctly assessing systemic risk in capital markets, particularly by considering the complex interconnections between financial institutions—that make the system more fragile than previously thought [1–5]. Indeed, direct exposures to bilateral contracts (through counterparty and roll-over risk) and indirect exposures to common assets (due to overlapping portfolios) stand for important channels of distress propagation in financial networks [6–10]. Thus, characterising the emerging network structure of financial systems is nowadays a scientific and institutional priority [11–17]. However, while financial institutions must disclose their aggregated exposures to other institutions or towards the market, detailed data on their single filing positions is almost often privacy-protected and thus inaccessible. For this reason, reconstructing the network structure from aggregated data is currently a widespread research topic [18–29]. Many techniques have been developed to reconstruct *monopartite* networks of bilateral exposures between financial institutions, whereas, methods to reconstruct the *bipartite* structure of stocks ownership by financial institutions are still little explored [30]—possibly because of lack of testing data. This despite the crucial importance of the issue: portfolio overlaps have the potential to trigger *fire sales*, i.e., downward spirals for illiquid asset prices due to self-reinforcing sell orders [31–35]. Moreover, fire sales spillovers create incentives to hoard liquidity, activating a spiral that can lead the financial system to freeze completely [36–40].

Reconstruction of monopartite networks of direct exposures between financial institutions (such as the in-

terbank lending market) from aggregated balance sheet information is typically achieved through maximum entropy techniques, that use the available information as constraints to be satisfied [18, 19]. The major drawback of these approaches is however that of generating unrealistic fully connected topologies, which moreover lead to systemic risk underestimation [20, 21]. Thus, several techniques have been developed to obtain sparse reconstructions [21–24], particularly by trying to guess how connection probabilities depend on aggregated exposures [27]. Notably, while these approaches usually explore the space of possible network densities, or directly use *ad-hoc* density values, a recently developed *bootstrapping* algorithm allows to obtain a close guess of the true link density by relying on small informative subsamples [41, 42]. The latter approach has then been turned into a statistically-grounded reconstruction procedure, based on assessing connection probabilities through a *configuration model* (CM) [43, 44], tailored on the estimated density and induced by the aggregated exposures used as *fitnesses* [45]—similarly to fitness-dependent network models [46]. This approach is then complemented with a *degree-corrected gravity model* (dcGM) [28] or with an *enhanced* CM (ECM) [29, 47] to place link weights.

When applied to networks of institutional portfolio holdings, reconstruction methods have to account for the bipartite structure of the system: there are two classes of nodes (institutions and stocks) and connections are established only between nodes belonging to different classes. Standard maximum entropy techniques have been extended to this context, with initial guess for matrix entries given by the *capital asset pricing model*

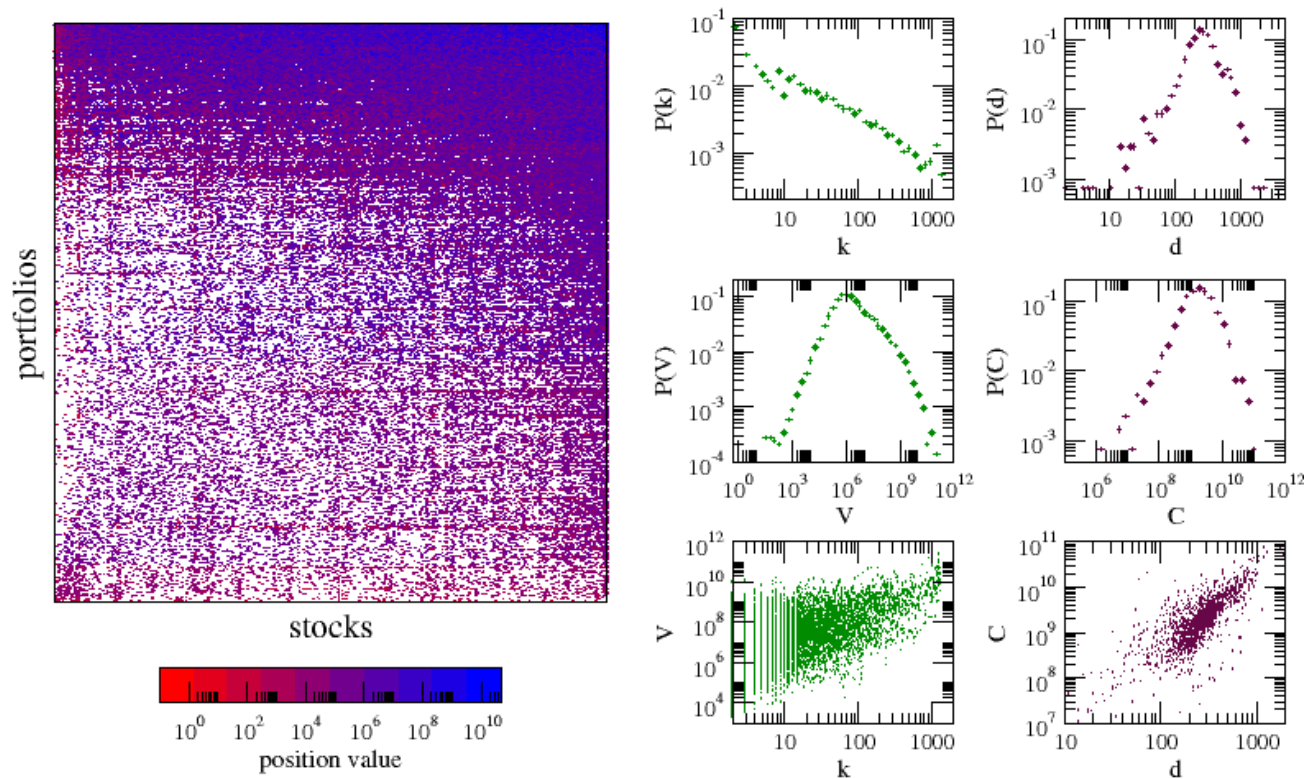


FIG. 1. Properties of our stock market data, with values expressed in dollar units: bipartite weighted adjacency matrix (left panel), distributions of degrees and strengths (upper right panels) and relation between degrees and strengths (bottom right panels). The linearity of the latter relation is at the basis of the ansatz of our method that  $x_i \propto V_i \forall i$  and  $y_\alpha \propto C_\alpha \forall \alpha$ .

(CAPM): investors choose their portfolio such that each position on a stock is proportional to that stock market value [48]. Recently, an extended maximum entropy framework constraining matrix entries to CAPM values (MECAPM) has been formalized [30]. Yet, all these approaches again end up generating almost fully connected networks, thus failing to reproduce the real network and underestimating risk [20, 33] (but this may also depend on the metric chosen, see [30]).

Given this state of the art, here we aim at overcoming the density issue for bipartite network reconstruction, by extending the *fitness-induced* CM (FiCM) approach outlined above that we recently introduced for monopartite networks. Using node strengths to represent aggregated balance sheet data, in a nutshell the method consists of a two step inference procedure: first, links presence is assessed through a *bipartite* CM (BiCM) [49] calibrated using the strengths as fitnesses, and then weights are placed with the dcGM. Whence, the name *fitness-induced* BiCM (or FiBiCM). To validate our method, we use a snapshot of the stock market taken from the Bloomberg terminal at 2014Q3 (see Fig. 1 for basic statistics, and the SI for more details). The datasets comprises  $N = 30257$  investors portfolios and  $M = 1370$  stocks (as collected from NASDAQ, NYSE and AMEX) and is represented as

a weighted undirected bipartite network: the generic element  $w_{i\alpha} = \pi_\alpha f_{i\alpha}$  is the value of stock  $\alpha$  held in portfolio  $i$ , and is given by the outstanding shares  $f_{i\alpha}$  times the stock price  $\pi_\alpha$ . The aggregated balance sheet information are then given by the nodes *strengths*, namely the market value of portfolio  $i$ ,  $V_i = \sum_\alpha w_{i\alpha}$ , and the market capitalization of stock  $\alpha$ ,  $C_\alpha = \sum_i w_{i\alpha}$ . Nodes *degrees* are instead given by the number of different stocks held by portfolio  $i$ ,  $k_i = \sum_\alpha a_{i\alpha}$ , and by the number of investors in stock  $\alpha$ ,  $d_\alpha = \sum_i a_{i\alpha}$  (where  $a_{i\alpha} = 1 - \delta_{[w_{i\alpha}, 0]}$ ). We denote by  $W = \sum_{i\alpha} w_{i\alpha}$  the total economic value in the market, and by  $L = \sum_{i\alpha} a_{i\alpha}$  the total number of connections (ownership relations) in the network. Since we have full information on this data, we will be able to precisely assess the accuracy of our reconstruction method.

We now proceed to a detailed explanation of the FiBiCM network reconstruction procedure. The aim is to find the optimal estimate for  $X(G_0)$ , the value of a property  $X$  for the real network  $G_0$ , on the basis of the limited available information on  $G_0$  itself: the total number of nodes  $N, M$  and links  $L$ , and the whole strength sequences  $\{V_i\}_{i=1}^N$  and  $\{C_\alpha\}_{\alpha=1}^M$ . Such quantities will act as constraints in the estimation procedure: we will consider  $G_0$  as drawn from the appropriate maximally random ensemble  $\Omega$  of bipartite graphs compatible with such

constraints, so that  $X(G_0)$  can be estimated as  $\langle X \rangle_\Omega$  (the average of  $X$  over the ensemble). As already mentioned, the method proceeds in two main steps.

I) We first reconstruct the binary topology of  $G_0$ . To this end, if we knew the degree for each node of the network, we could use directly the BiCM [49] to generate an ensemble  $\Omega$  of maximally random networks such that the ensemble average of the node degrees are constrained to the values observed in  $G_0$ :  $\langle k_i \rangle_\Omega \equiv k_i \forall i$  and  $\langle d_\alpha \rangle_\Omega \equiv d_\alpha \forall \alpha$ . This would lead to a probability distribution over  $\Omega$  of all possible binary bipartite graphs, defined via a set of Lagrange multipliers  $\{x_i\}_{i=1}^N$  and  $\{y_\alpha\}_{\alpha=1}^M$  (one for each node) associated to the constraints. Once all multipliers are found, the BiCM would reduce to having a link between nodes  $i$  and  $\alpha$  with probability:

$$p_{i\alpha} = \frac{x_i y_\alpha}{1 + x_i y_\alpha}, \quad (1)$$

independently of all other links. Here, however, we are studying the case where node degrees are unknown, yet we know the total number  $L$  of links. Thus, while we cannot directly use the BiCM, we can resort to the *fitness* model [45] and assume the network topology to be determined by intrinsic node properties, the fitnesses. This approach has been successfully used in the past to model several economic and financial networks, by assuming a connection between fitnesses and Lagrange multipliers [46, 50, 51]. Thus, as in the case of interbank networks [28, 29], we make the ansatz that the strengths represent node-specific fitnesses induced by their degrees, and are thus proportional to the degree-induced Lagrange multipliers of the BiCM:  $x_i \equiv \sqrt{z_V} V_i \forall i$  and  $y_\alpha \equiv \sqrt{z_C} C_\alpha \forall \alpha$  (see Fig. 1 and the discussion ahead). Thanks to this assumption, our task reduces to find these proportionality constants, which is achieved by equating the average number of links of a graph belonging to  $\Omega$  to the (known) total number  $L$  of links in  $G_0$ :

$$\langle L \rangle_\Omega \equiv \sum_i \sum_\alpha \frac{z V_i C_\alpha}{1 + z V_i C_\alpha} = L \quad (2)$$

where we have defined  $z = \sqrt{z_V z_C}$ . Since the strengths are known, eq. (2) is an algebraic equation in  $z$  with a single solution for  $z > 0$ , which is then used to estimate the linking probabilities of eq. (1):

$$p_{i\alpha} = \frac{z V_i C_\alpha}{1 + z V_i C_\alpha} \equiv \langle \tilde{a}_{i\alpha} \rangle_\Omega \quad \forall (i, \alpha). \quad (3)$$

Here,  $\tilde{a}_{i\alpha}$  is the generic matrix element of a network drawn from  $\Omega$ .

II) We then reconstruct the weighted topology of  $G_0$ . The formal approach [47] would consist in maximizing the entropy with constraints given by both nodes strengths and degrees (using for the latter either the empirical values or their estimates from step I—as done in [29]). Yet, this procedure may become unfeasible for

large networks, as it requires the solution of  $2(N + M)$  coupled nonlinear equations. Thus, here we resort to the simple dcGM prescription proposed in [28], and extend it to bipartite networks. Indeed, standard gravity models [18, 20] work only for fully connected networks, and in our context would basically assign weights exactly like in the CAPM as  $\tilde{\omega}_{i\alpha} = V_i C_\alpha / W$ . However, when the topology is determined by nontrivial connection probabilities, in order to reproduce the observed strengths the weights of individual links have to be determined as:

$$\tilde{w}_{i\alpha} = \frac{V_i C_\alpha}{W p_{i\alpha}} \tilde{a}_{i\alpha} = (z^{-1} + V_i C_\alpha) \frac{\tilde{a}_{i\alpha}}{W}, \quad (4)$$

Notably, this prescription ensures that the expected value of the reconstructed link weight is equal to the CAPM value:  $\langle \tilde{w}_{i\alpha} \rangle_\Omega \equiv \tilde{\omega}_{i\alpha} \forall (i, \alpha)$ . Additionally, the expected value of node strengths are equal to the observed values, whatever the underlying topology [29]. In this respect, it is useful to point out now the relation between our FiBiCM reconstruction technique and the MECAPM (see the SI for more details). Indeed, both approaches return expected link weights equal to CAPM values. However, in the latter case connection probabilities read  $\tilde{\omega}_{i\alpha} / (1 + \tilde{\omega}_{i\alpha})$ , which is the special case  $z = 1$  of eq. (3). As for this value of  $z$  connection probabilities become very close to 1, we see that again the formal entropy maximization without constraining the network connectivity distributes weights as evenly as possible, and so generates a very dense network. Now, while it can be difficult to impose the observed density *ex-ante* inside the function to maximize, the stratagem we resort to overcome this issue is to impose it *ex-post* through the parameter  $z$  and eq. (2), and to use a self-consistent gravity approach to adjust and redistribute link weights.

We now move to validation of the FiBiCM algorithm. To this end, we consider three different kinds of performance metrics: topological, statistical and financial indicators. First, in order to check whether the reconstructed ensemble  $\Omega$  is representative for the real network, we compare for all nodes the empirical degrees  $k_i$  and  $d_\alpha$  with  $\langle k_i \rangle_\Omega = \sum_\alpha p_{i\alpha}$  and  $\langle d_\alpha \rangle_\Omega = \sum_i p_{i\alpha}$  estimated through our method. As Figure 2 shows, this results in a scattered cloud around the identity, whose behavior reflects the high correlation between these values. Having checked that the method works for single node properties, we now move to higher order properties related to node pairs, and consider the bipartite average nearest neighbors degree [49]:  $d_i^{nn} = \sum_\alpha a_{i\alpha} d_\alpha / k_i$  and  $k_\alpha^{nn} = \sum_i a_{i\alpha} k_i / d_\alpha$ , that is, the arithmetic mean of the degrees of neighboring nodes (belonging to the opposite layer of the bipartite network). Figure 3 shows that we can correctly reproduce the behavior of this quantity, by accurately interpolating the observed clouds of values. Note that the MECAPM method in this case would completely fail to reproduce the observed topological properties, precisely because it generate a very dense

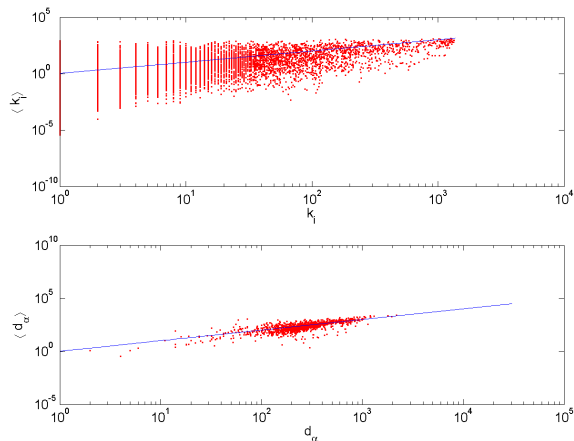


FIG. 2. Scatter plot of observed (red points) and expected (blue points) degrees for portfolios (top panel) and stocks (bottom panel).

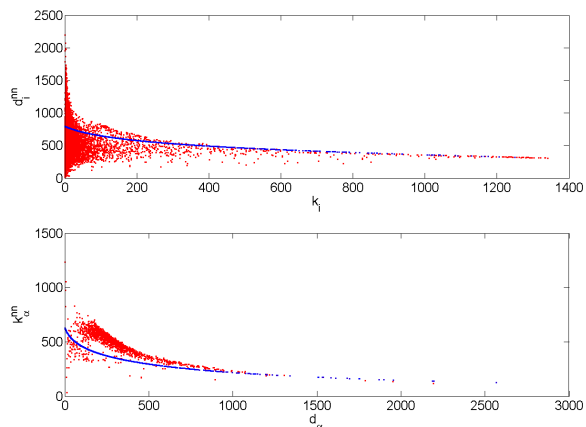


FIG. 3. Scatter plot of observed (red points) and expected (blue points) average nearest neighbors degrees of portfolios (top panel) and stocks (bottom panel).

network (see the SI).

Having explored topological indicators, we move further to statistical indices, which are intended to test the FiBiCM in reproducing the “details” of the observed network structure. In particular, we aim at quantifying the ability of the method to correctly predict the presence of a link between two nodes when that link is actually there in the real network (a *true positive*) and the absence of a link when that link is missing in the real network (a *true negative*). As explained in the SI, the occurrence of these events allows to define standard statistical measures for the performance of our method when used as a binary classification test: *true positive rate* (TPR), *specificity* (SPC), *positive predicted value* (PPV) and *accuracy* (ACC). Table I sums up the values of these quantities for the FiBiCM and MECAPM algorithm. In order to

	TPR	SPC	PPV	ACC
FiBiCM	0.21	0.99	0.21	0.98
MECAPM	0.99	0.024	0.010	0.034

TABLE I. Summary of statistical indicators for FiBiCM and MECAPM algorithm.

interpret properly the results of this test, we again have to recall that while our method reproduces the observed link density  $c = L/(NM) \simeq 0.01$  (since  $\langle L \rangle = L$ ), the MECAPM returns an estimate  $c' \simeq 0.98$ : the reconstructed network is almost fully connected. As a trivial consequence, MECAPM correctly identifies all the existing links and achieves a very high TPR. However, this fact also represents its major drawback, as MECAPM fails in identifying the nonexisting links and achieves a very low SPC. Overall, the proportion of true guesses among the total number of cases examined (ACC) is very low for MECAPM. On the other hand, FiBiCM can correctly guess almost all nonexisting links, but at the same time also places a good percentage of existing links, resulting in an overall very high accuracy.

Lastly, we consider financial indicators to compare the level of systemic risk in the reconstructed network with that of the original system. As risk metric, we follow [30] and adopt the systemicness index  $S$  as a measure for the vulnerability of financial institutions [34] (see the SI for definitions and details on the following discussion). Figure 4 shows that the FiBiCM can reproduce well the empirical systemicness especially for high values of institutional capitalization  $V$ . This is because the method, besides reproducing the aggregated strengths, does particularly well in reproducing the largest weights of the network—which are given by the positions of the biggest, and thus more important, institutions. Instead, for small and medium institutions, systemicness is usually overestimated, yet our reconstruction approach can still be useful in providing an upper bound for systemic risk. Concerning MECAPM, notably its predicted systemicness values are very similar to those obtained by our FiBiCM, thus the two methods perform equally in terms of this risk measure. This happens because of the mathematical definition of  $\langle S_i \rangle$  in the two ensembles, which turns out to be only weakly dependent on the topological details of the network: what matters the most are the aggregate node strengths, hence any reconstruction algorithm capable of correctly reproducing them is likely to achieve the same performance for systemicness, irrespectively of its performance regarding purely structural quantities. This feature may however represents an important drawback of the chosen financial indicator, as generally systemic risk is considered to be highly influenced by the network topology. For instance, in [33] it is shown that the probability of financial contagion in

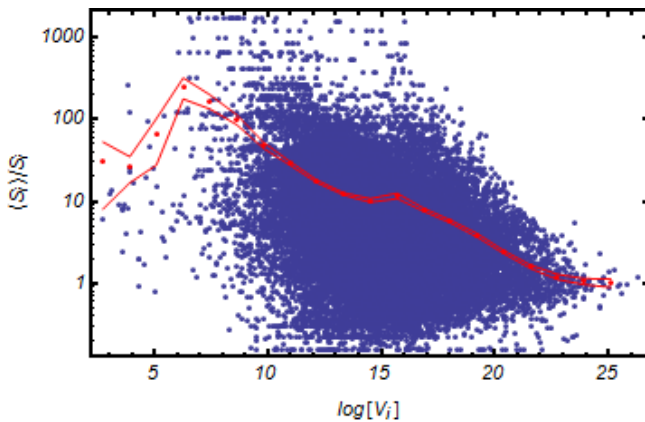


FIG. 4. Performance of the FiBiCM in reproducing nodes systemicness: scatter plot of capitalization  $V$  versus the ratio between estimated and empirical systemicness for each institution in the network. Red points represent average values resulting from a logarithmic binning of the horizontal axis, and the continuous lines show the confidence interval corresponding to one standard deviation for such averages. Note that  $\langle S_i \rangle_\Omega / S_i \simeq 1$  (which means an accurate estimate) is achieved especially for high  $V_i$  values.

stock markets strongly depends on connectivity, being minimal for both the very sparse and the very dense configurations and maximal for intermediate density values (while the extent of contagion is a monotonic function of the density). Also in [52] the heterogeneity of portfolios diversifications is shown to affect the extent and coordination of feedback and contagion effects. Nevertheless, we use systemicness here as it represents an intuitive and easily implementable measure and, more importantly, is considered nowadays as one of the more robust risk indicator for individual financial institutions.

In conclusion, we have shown that the FiBiCM has the same performance of the MECAPM for what concerns financial indicators, but generally outperforms it in reproducing statistical and topological properties. We remark however that the applicability of our method strongly depends on the accuracy of the ansatz of whether the BiCM induced by node strengths is able to provide good estimates for the unknown degrees. The validity of such ansatz can be assessed in any particular case study by comparing node strengths versus their degrees, also in small subsets of the network where full information is available. In any event, the ansatz derives from a simple argument, corroborated by similar evidence found in the analysis of several economic and financial networks [28, 29, 46, 50, 51]: the most important a node, the bigger we expect its degree to be. More technically, any measure of importance of a node is likely to be a monotonic function of the Lagrange multiplier that controls the degree of that node. If such a measure is strictly positive, then its simplest dependency on the multiplier is linear. Another

important feature of our method is that the probability of generating a graph factorizes into the probabilities of connecting the different pairs of nodes. This aspect (known as *independence of dyads*) could be seen as making the method inherently inadequate to reproduce, for instance, community or core-periphery structures. However, such independence is not postulated by us at any stage; rather, it emerges naturally from the enforcement of purely local constraints: the maximum-entropy method automatically generates independent dyads as the unbiased solution to the inference problem. Paradoxically, introducing (more realistic) dependencies among dyads would result in a biased inference.

Finally, we remark that the effectiveness of our method has still to be asserted on different datasets, that also contain the temporal dynamics of the market and encompass bubbles and crises. Yet, we believe that our method to reconstruct the statistical properties of a network when only partial information is available addresses a key open problem, and thus will represent a valuable tool both for the wide community of complex systems scientists and for institutional regulators trying to ensure the stability of the financial system.

This work was supported by the EU projects MULTIPLEX (FP7-ICT, grant n. 317532), SIMPOL (FP7-ICT, grant n. 610704) and DOLFINI (H2020-EU.1.2.2., grant n. 640772). We thank Stefano Battiston for useful discussions, Riccardo Di Clemente for data collection, and the Italian PNR project CRISIS-Lab for granting access to the Bloomberg terminal.

---

\* giulio.cimini@imtlucca.it

- [1] J. A. Chan-Lau, M. Espinosa, K. Giesecke, and J. A. Solé, *Assessing the Systemic Implications of Financial Linkages*, Tech. Rep. (IMF Global Financial Stability Report, 2009).
- [2] M. K. Brunnermeier, *Journal of Economic Perspectives* **23**, 77 (2009).
- [3] A. Krause and S. Giansante, *Journal of Economic Behavior & Organization* **83**, 583 (2012).
- [4] S. Kapadia, M. Drehmann, J. Elliott, and G. Sterne, “Liquidity risk, cash flow constraints, and systemic feedbacks,” in *Quantifying Systemic Risk* (University of Chicago Press, 2012) pp. 29–61.
- [5] S. Battiston, G. Caldarelli, R. May, T. Roukny, and J. E. Stiglitz, SSRN:2594028 (2015).
- [6] F. Allen and D. Gale, *Journal of Political Economy* **108**, 1 (2000).
- [7] L. Eisenberg and T. H. Noe, *Management Science* **47**, 236 (2001).
- [8] P. Gai, A. Haldane, and S. Kapadia, *Journal of Monetary Economics* **58**, 453 (2011).
- [9] A. G. Haldane and R. M. May, *Nature* **469**, 351 (2011).
- [10] D. Acemoglu, A. Ozdaglar, and A. Tahbaz-Salehi, *American Economic Review* **105**, 564 (2015).

- [11] M. Boss, H. Elsinger, M. Summer, and S. Thurner, *Quantitative Finance* **4**, 677 (2004).
- [12] G. Iori, S. Jafarey, and F. G. Padilla, *Journal of Economic Behavior & Organization* **61**, 525 (2006).
- [13] H. Elsinger, A. Lehar, and M. Summer, *Management Science* **52**, 1301 (2006).
- [14] E. W. Nier, J. Yang, T. Yorulmazer, and A. Alentorn, *Network Models and Financial Stability*, Bank of England Working Paper 346 (2008).
- [15] S. Battiston, M. Puliga, R. Kaushik, P. Tasca, and G. Caldarelli, *Scientific Reports* **2**, 541 (2012).
- [16] S. Battiston, J. D. Farmer, A. Flache, D. Garlaschelli, A. G. Haldane, H. Heesterbeek, C. Hommes, C. Jaeger, R. May, and M. Scheffer, *Science* **351**, 818 (2016).
- [17] M. Bardoscia, S. Battiston, F. Caccioli, and G. Caldarelli, arXiv:1602.05883 (2016).
- [18] S. J. Wells, *Financial Interlinkages in the United Kingdom's Interbank Market and the Risk of Contagion*, Bank of England Working Paper 230 (Bank of England, 2004).
- [19] C. Upper, *Journal of Financial Stability* **7**, 111 (2011).
- [20] P. E. Mistrulli, *Assessing Financial Contagion in the Interbank Market: Maximum Entropy versus Observed Interbank Lending Patterns*, Temi di discussione (Economic working papers) 641 (Bank of Italy, Economic Research and International Relations Area, 2007).
- [21] I. Mastromatteo, E. Zarinelli, and M. Marsili, *Journal of Statistical Mechanics: Theory and Experiment* **2012**, P03011 (2012).
- [22] M. Drehmann and N. Tarashev, *Journal of Financial Intermediation* **22**, 586 (2013).
- [23] G. Halaj and C. Kok, *Computational Management Science* **10**, 157 (2013).
- [24] K. Anand, B. Craig, and G. von Peter, *Filling in the Blanks: Network Structure and Interbank Contagion*, Discussion Papers 02/2014 (Deutsche Bundesbank Research Centre, 2014).
- [25] T. A. Peltonen, M. Rancan, and P. Sarlin, *Interconnectedness of the Banking Sector as a Vulnerability to Crises*, ECB Working Paper 1866 (European Central Bank, 2015).
- [26] P. Baral and J. P. Figue, *Estimation of Bilateral Exposures - A Copula Approach*, Mimeo (2012).
- [27] M. Montagna and T. Lux, *Contagion Risk in the Interbank Market: A Probabilistic Approach to Cope with Incomplete Structural Information*, Kiel Working Papers (Kiel Institute for the World Economy, 2014).
- [28] G. Cimini, T. Squartini, D. Garlaschelli, and A. Gabrielli, *Scientific Reports* **5**, 15758 (2015).
- [29] G. Cimini, T. Squartini, A. Gabrielli, and D. Garlaschelli, *Physical Review E* **92**, 040802 (2015).
- [30] D. Di Gangi, F. Lillo, and D. Pirino, arXiv:1509.00607 (2015).
- [31] A. Shleifer and R. W. Vishny, *Fire Sales in Finance and Macroeconomics*, Tech. Rep. (National Bureau of Economic Research, 2010).
- [32] T. Adrian and H. S. Shin, *Journal of Financial Intermediation* **19**, 418 (2010).
- [33] F. Caccioli, M. Shrestha, C. Moore, and J. D. Farmer, *Journal of Banking & Finance* **46**, 233 (2014).
- [34] R. Greenwood, A. Landier, and D. Thesmar, *Journal of Financial Economics* **115**, 471 (2015).
- [35] S. Gualdi, G. Cimini, K. Primicerio, R. D. Clemente, and D. Challet, arXiv:1603.05914 (2016).
- [36] D. W. Diamond and R. G. Rajan, *Fear of Fire Sales and the Credit Freeze*, Working Paper 14925 (National Bureau of Economic Research, 2009).
- [37] J. M. Berrospide, *Bank Liquidity Hoarding and the Financial Crisis: An Empirical Evaluation*, Finance and Economics Discussion Series 03 (Board of Governors of the Federal Reserve System (U.S.), 2013).
- [38] D. Gale and T. Yorulmazer, *Theoretical Economics* **8**, 291 (2013).
- [39] V. V. Acharya and O. Merrouche, *Review of Finance* **17**, 107 (2013).
- [40] S. Gabrieli and G. Co-Pierre, *A Network View on Interbank Market Freezes*, Working papers 531 (Banque de France, 2014).
- [41] N. Musmeci, S. Battiston, G. Caldarelli, M. Puliga, and A. Gabrielli, *Journal of Statistical Physics* **151**, 720 (2013).
- [42] G. Cimini, T. Squartini, N. Musmeci, M. Puliga, A. Gabrielli, D. Garlaschelli, S. Battiston, and G. Caldarelli, "Social informatics: Socinfo 2014 international workshops, barcelona, spain, november 11, 2014, revised selected papers," (Springer International Publishing, 2015) Chap. Reconstructing Topological Properties of Complex Networks Using the Fitness Model, pp. 323–333.
- [43] J. Park and M. E. J. Newman, *Physical Review E* **70**, 066117 (2004).
- [44] T. Squartini and D. Garlaschelli, *New Journal of Physics* **13**, 083001 (2011).
- [45] G. Caldarelli, A. Capocci, P. De Los Rios, and M. A. Muñoz, *Phys. Rev. Lett.* **89**, 258702 (2002).
- [46] D. Garlaschelli and M. I. Loffredo, *Phys. Rev. Lett.* **93**, 188701 (2004).
- [47] R. Mastrandrea, T. Squartini, G. Fagiolo, and D. Garlaschelli, *New Journal of Physics* **16**, 043022 (2014).
- [48] J. Mossin, *Econometrica* **34**, 768 (1966).
- [49] F. Saracco, R. Di Clemente, A. Gabrielli, and T. Squartini, *Scientific Reports* **5**, 10595 (2015).
- [50] D. Garlaschelli, S. Battiston, M. Castri, V. D. Servidio, and G. Caldarelli, *Physica A: Statistical Mechanics and its Applications* **350**, 491 (2005).
- [51] G. De Masi, G. Iori, and G. Caldarelli, *Phys. Rev. E* **74**, 066112 (2006).
- [52] F. Corsi, S. Marmi, and F. Lillo, SSRN:2278298 (2013).

## SUPPLEMENTARY INFORMATION

### Dataset

The dataset we analyse in the paper consists of a snapshot of the long positions held by investors over securities traded on the world's major stock exchanges: NASDAQ, NYSE and AMEX. Data were taken from the Bloomberg terminal (<http://www.bloomberg.com/professional/hardware/>) at 2014Q3, and comprise  $M = 5501$  securities or stocks and  $N = 91247$  investors or portfolios. Each stock is uniquely identified by its ticker symbol, and each investor by the portfolio name (as investors may own more than one portfolio). Among the various metadata associated to a given portfolio, we have its status: either N-P (corresponding to the main portfolio of an institution), N-C (a sub-portfolio of an N-P portfolio) or Y (a private investor). In this respect, since ownership information of N-C portfolios is contained in that of main N-P portfolios, in our analysis we will only consider N-C and Y portfolios (and thus we reduce to  $N = 74375$ ). Then, for each stock  $\alpha$  we have the list of owner portfolios  $\{i\}$ , with the following information: filing position for the number of shares outstanding  $f_{i\alpha}$ , value of these shares  $w_{i\alpha} = \pi_\alpha f_{i\alpha}$  (where  $\pi_\alpha$  is the stock price), and percentage  $o_{i\alpha}$  that these shares represent in the total issued shares of  $\alpha$ . Now, if for a security the percentage of total outstanding shares in our dataset (as computed over N-P and Y portfolios), namely  $\sum_j o_{j\alpha}$ , is smaller than 100%, it means that some of the shares issued by the respective corporation are held by the corporation itself and have no exercisable rights. In this case, for that security the total trade volume in the market may not be representative for its total market capitalization. As this feature can introduce biases in the dataset, we only consider stocks with 100% outstanding shares. In this way, we obtain a reduced dataset of  $N = 30257$  portfolios and  $M = 1370$  stocks, whose *strengths* (total value of portfolios and market capitalization of stocks) can be consistently computed internally to the dataset.

### The MECAPM method

The MECAPM method combines the constrained entropy-maximization (ME) technique and the estimation for the single link weights  $w_{i\alpha}$  as for the CAPM model [30]. In particular, the prescription for weights reads

$$\langle w_{i\alpha} \rangle_{\text{CAPM}} = \frac{V_i C_\alpha}{W}. \quad (5)$$

This formula for the expectation value can be combined with ME within the ERG theoretical framework [43, 44]. Indeed, the MECAPM model is obtained by constraining the whole set of weights of a given bipartite undirected weighted network  $\mathbf{W}$ . In this particular case, the probability distribution of the considered network factorizes as the product of pair-specific geometric probability distributions

$$P(\mathbf{W}) = \prod_i \prod_\alpha q_{i\alpha}^{w_{i\alpha}} (1 - q_{i\alpha}). \quad (6)$$

In this context, the generic weight  $w_{i\alpha}$  is interpreted as a sum of unitary links, each behaving as an independent Bernoulli random variable. Thus, each pair-specific probability distribution is characterized by a quantity  $q_{i\alpha}$ , namely the probability that the corresponding unitary link between nodes  $i$  and  $\alpha$  is present. The  $N \cdot M$  unknown parameters  $q_{i\alpha}$  ( $i = 1 \dots N$  and  $\alpha = 1 \dots M$ ) can be estimated by exploiting the likelihood condition [44]

$$\langle w_{i\alpha} \rangle_{\text{CAPM}} = \frac{q_{i\alpha}}{1 - q_{i\alpha}}. \quad (7)$$

As a result, one gets

$$q_{i\alpha} = \frac{\langle w_{i\alpha} \rangle_{\text{CAPM}}}{1 + \langle w_{i\alpha} \rangle_{\text{CAPM}}} = \frac{V_i C_\alpha / W}{1 + V_i C_\alpha / W}. \quad (8)$$

For our dataset, such values are typically very high. In fact, although their range is  $[5 \cdot 10^{-5}, 1]$ , their distribution is characterized by an average value of  $\bar{q} \simeq 0.97$  and a standard deviation of  $\sigma_q \simeq 0.091$ . Thus, their variation coefficient is  $\sigma_q / \bar{q} \simeq 0.093$ , indicating that the average faithfully represents the distribution of values. In contrast, the probability coefficients computed with the FiBiCM vary in  $[10^{-12}, 1]$ , their average value is  $\bar{p} \simeq 0.01$  (coinciding with the network density of links) and their standard deviation is  $\sigma_p \simeq 0.057$ . In this case, the variation coefficient is  $\sigma_p / \bar{p} > 5$ , indicating that the average is not representative of the distribution of values, which is therefore widespread over the corresponding domain.

## Reconstruction performance indicators

### Topological indicators

The first family of indicators consists of quantities providing information on the structural organization of a given network. In particular, we consider 1) the *degree* of, respectively, portfolios and stocks,  $k_i(\mathbf{A}) = \sum_{\alpha} a_{i\alpha}$  and  $d_{\alpha}(\mathbf{A}) = \sum_i a_{i\alpha}$ , and 2) the *average nearest neighbors degree* of portfolios and stocks [49]

$$d_i^{nn}(\mathbf{A}) = \frac{\sum_{\alpha} a_{i\alpha} d_{\alpha}}{k_i}, \quad k_{\alpha}^{nn}(\mathbf{A}) = \frac{\sum_i a_{i\alpha} k_i}{d_{\alpha}} \quad (9)$$

and compared them with their values estimated within the FiBiCM ensemble, namely 1)  $\langle k_i \rangle = \sum_{\alpha} p_{i\alpha}$  and  $\langle d_{\alpha} \rangle = \sum_i p_{i\alpha}$ , and 2)

$$\langle d_i^{nn} \rangle = \frac{\sum_{\alpha} p_{i\alpha} \langle d_{\alpha} \rangle}{\langle k_i \rangle}, \quad \langle k_{\alpha}^{nn} \rangle = \frac{\sum_i p_{i\alpha} \langle k_i \rangle}{\langle d_{\alpha} \rangle}. \quad (10)$$

Concerning the MECAPM method, its predictions can be estimated by considering a very dense network (as justified above). In this case, we obtain  $\langle k_i \rangle_{\text{MECAPM}} \simeq \langle k_{\alpha}^{nn} \rangle_{\text{MECAPM}} \simeq M$  and  $\langle d_{\alpha} \rangle_{\text{MECAPM}} \simeq \langle d_i^{nn} \rangle_{\text{MECAPM}} \simeq N$ .

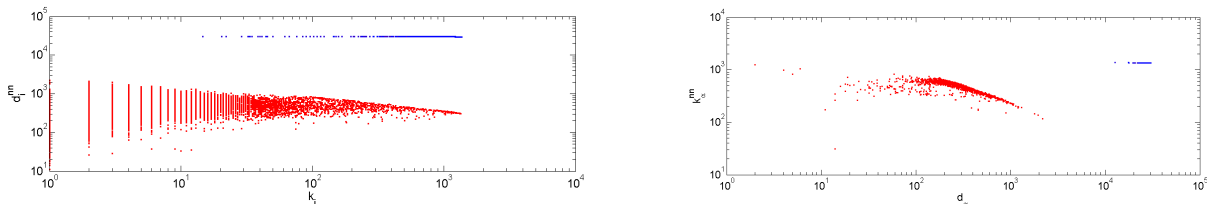


FIG. S1. Comparison between observed (red points) and expected (blue points) average nearest neighbors degree of portfolios (left panel) and stocks (right panel). Expected values have been computed by running the MECAPM algorithm: the flat trends reflect the high link-density of the MECAPM-induced reconstruction, not compatible with the real network structure.

### Statistical indicators

The second family of indicators is usually represented by the so-called *confusion matrix*. The latter is a  $4 \times 4$  matrix whose entries represent the number of *true positives*, *true negatives*, *false positives* and *false negatives*. We now briefly explain how these concepts apply to our case.

Reconstructing a network  $\mathbf{W}$  means providing an algorithm to estimate the *presence* and the *weight* of the links constituting the network. If, for simplicity, we limit our analysis to the binary structure only (represented by the binary matrix  $\mathbf{A}$ , with  $a_{i\alpha} = 1 - \delta_{[w_{i\alpha}, 0]}$ ), reconstruction means “guessing” the topological structure of the given network, i.e., the position of 0s and 1s. Thus, for each entry of the reconstructed matrix, four different situations are possible: **a)**  $a_{i\alpha} = 1$  and we correctly predict  $\tilde{a}_{i\alpha} = 1$ : we have a *true positive*; **b)**  $a_{i\alpha} = 1$  but we predict  $\tilde{a}_{i\alpha} = 0$ : we have a *false negative*; **c)**  $a_{i\alpha} = 0$  and we correctly predict  $\tilde{a}_{i\alpha} = 0$ : we have a *true negative*; **d)**  $a_{i\alpha} = 0$  but we predict  $\tilde{a}_{i\alpha} = 1$ : we have a *false positive*.

Now, given the original matrix  $\mathbf{A}$  and the reconstructed matrix  $\tilde{\mathbf{A}}$ , we can straightforwardly count the total number of true positives as the point-wise product of the two matrices:

$$TP = \sum_i \sum_{\alpha} a_{i\alpha} \tilde{a}_{i\alpha}. \quad (11)$$

Similarly, the total number of true negatives is:

$$TN = \sum_i \sum_{\alpha} (1 - a_{i\alpha})(1 - \tilde{a}_{i\alpha}) \quad (12)$$

From these quantities, the total number of false negatives is obtained simply as

$$FN = L - TP, \quad (13)$$

(where  $L$  is total number of observed links), and the total number of false positives as

$$FP = (N \cdot M - L) - TN. \quad (14)$$

whose first addendum counts how many 0s are observed in the real matrix  $\mathbf{A}$ .

The information provided by  $TP$ ,  $FN$ ,  $TN$  and  $FP$  can be further refined by combining them into four indices. *Sensitivity* (or *true positive rate*) is the percentage of 1s that are correctly placed in the reconstructed matrix:

$$TPR = \frac{TP}{TP + FN} = \frac{TP}{L}. \quad (15)$$

*Specificity* (or *true negative rate*) is by contrast the percentage of 0s that are correctly recovered by our method:

$$SPC = \frac{TN}{FP + TN} = \frac{TN}{(N \cdot M - L)}. \quad (16)$$

*Precision* (or *positive predicted value*) measures the performance of the reconstruction procedure in correctly placing 1s with respect to the total number of predicted 1s:

$$PPV = \frac{TP}{TP + FP}. \quad (17)$$

Finally, *accuracy* measures the overall performance of the reconstruction in correctly placing both 1s and 0s:

$$ACC = \frac{TP + TN}{TP + TN + FP + FN} = \frac{TP + TN}{(N \cdot M)}. \quad (18)$$

Since both the FiBiCM and the MECAPM method deal with an entire ensemble of candidate matrices  $\tilde{\mathbf{A}}$ , we are interested in estimating the expected number of errors we can make. To this end, we can calculate the ensemble average of the aforementioned indices as follows:

$$\langle TP \rangle = \sum_i \sum_\alpha a_{i\alpha} p_{i\alpha}; \quad \langle FN \rangle = L - \langle TP \rangle; \quad \langle TN \rangle = \sum_i \sum_\alpha (1 - a_{i\alpha})(1 - p_{i\alpha}); \quad \langle FP \rangle = (N \cdot M - L) - \langle TN \rangle, \quad (19)$$

$$\langle TPR \rangle = \frac{\langle TP \rangle}{L}; \quad \langle SPC \rangle = \frac{\langle TN \rangle}{(N \cdot M - L)}; \quad \langle PPV \rangle = \frac{\langle TP \rangle}{\langle TP \rangle + \langle FP \rangle}; \quad \langle ACC \rangle = \frac{\langle TP \rangle + \langle TN \rangle}{(N \cdot M)}, \quad (20)$$

Note that for the FiBiCM, as a consequence of the density tuning we have  $\langle L \rangle = L$ , and thus PPV and TPR coincide. In fact  $\langle TN \rangle = (N \cdot M - L) - \langle L \rangle + \langle TP \rangle = (N \cdot M - 2L) + \langle TP \rangle$  and  $\langle TP \rangle + \langle FP \rangle = \langle TP \rangle + (N \cdot M - L) - \langle TN \rangle = L$ .

The predictions of the MECAPM method can be obtained instead by considering  $q_{i\alpha} \simeq 0.97 \forall i, \alpha$  (i.e., all the MECAPM coefficients are equal to their average value) and replacing  $p_{i\alpha}$  with  $q_{i\alpha}$  in eqs. (19). In this case, we have that  $\langle TP \rangle_{\text{MECAPM}} \simeq 0.97L$ ,  $\langle FN \rangle_{\text{MECAPM}} \simeq 0.03L$ ,  $\langle TN \rangle_{\text{MECAPM}} \simeq 0.03(N \cdot M - L)$  and  $\langle FP \rangle_{\text{MECAPM}} \simeq 0.97(N \cdot M - L)$ . Thus,

$$\langle TPR \rangle_{\text{MECAPM}} \simeq 0.97; \quad \langle SPC \rangle_{\text{MECAPM}} \simeq 0.03; \quad \langle PPV \rangle_{\text{MECAPM}} \simeq \frac{L}{(N \cdot M)}; \quad \langle ACC \rangle_{\text{MECAPM}} \gtrsim \frac{L}{(N \cdot M)}. \quad (21)$$

#### Financial indicators

The last family of indicators consists of indices aimed at providing information on the systemic risk for a given financial network but at the level of single institutions. We follow [30] and adopt the *systemicness* index of [34]:

$$S_i = \Gamma_i \frac{V_i}{E} B_i r_i \quad (22)$$

which can be compared with its estimated counterpart  $\langle S_i \rangle$  via the ratio  $\langle S_i \rangle / S_i$ . After some algebraic manipulations [30], such a ratio can be rewritten as

$$\frac{\langle S_i \rangle}{S_i} = \frac{\sum_j \sum_\alpha \langle w_{i\alpha} w_{j\alpha} \rangle}{\sum_j \sum_\alpha w_{i\alpha} w_{j\alpha}} = \frac{\sum_\alpha \langle w_{i\alpha}^2 \rangle + \sum_{j \neq i} \langle w_{i\alpha} \rangle \langle w_{j\alpha} \rangle}{\sum_\alpha w_{i\alpha} C_\alpha} \quad (23)$$

which also coincides with the ratio between estimated and real *vulnerability* of the same institution [34]. This expression can be further simplified by considering that

$$\langle w_{i\alpha} \rangle = \frac{V_i C_\alpha}{W}, \quad \langle w_{i\alpha}^2 \rangle = \left( \frac{V_i C_\alpha}{W p_{i\alpha}} \right)^2 p_{i\alpha}; \quad (24)$$

thus, we end up with the expression

$$\frac{\langle S_i \rangle}{S_i} = \frac{\sum_\alpha \left( \frac{V_i C_\alpha}{W p_{i\alpha}} \right)^2 p_{i\alpha} + \frac{V_i C_\alpha}{W} \left[ C_\alpha - \frac{V_i C_\alpha}{W} \right]}{\sum_\alpha w_{i\alpha} C_\alpha}. \quad (25)$$

In the case of the MECAPM method, we have

$$\langle w_{i\alpha} \rangle_{\text{MECAPM}} = \frac{V_i C_\alpha}{W}, \quad \langle w_{i\alpha}^2 \rangle_{\text{MECAPM}} = \frac{V_i C_\alpha}{W} \left( 1 + 2 \frac{V_i C_\alpha}{W} \right) \quad (26)$$

which leads to

$$\frac{\langle S_i \rangle_{\text{MECAPM}}}{S_i} = \frac{\sum_\alpha \frac{V_i C_\alpha}{W} \left[ 1 + C_\alpha + \frac{V_i C_\alpha}{W} \right]}{\sum_\alpha w_{i\alpha} C_\alpha}. \quad (27)$$

Interestingly, in both cases the term  $\frac{V_i C_\alpha^2}{W}$  dominates in the numerator, thus leading to the simplification

$$\frac{\langle S_i \rangle}{S_i} = \frac{\langle S_i \rangle_{\text{MECAPM}}}{S_i} \simeq \frac{\sum_\alpha \frac{V_i C_\alpha^2}{W}}{\sum_\alpha w_{i\alpha} C_\alpha} = \frac{\sum_\alpha \langle w_{i\alpha} \rangle C_\alpha}{\sum_\alpha w_{i\alpha} C_\alpha} \quad (28)$$

since  $\langle w_{i\alpha} \rangle = \langle w_{i\alpha} \rangle_{\text{MECAPM}}$ . This further implies that, among the reconstruction methods reproducing the constraints represented by the strengths, the ones which better reproduce the systemicness index are those better reproducing the observed weights. As discussed in the main text, the prescription  $\langle w_{i\alpha} \rangle = \langle w_{i\alpha} \rangle_{\text{MECAPM}} = V_i C_\alpha / W$ , beside ensuring that  $\langle C_\alpha \rangle = C_\alpha$ , is particularly successful in reproducing the largest weights of our network—whence the correct estimates for the systemicness of large institutions.